Supplementary Information

Structural and dynamic studies of $Pr(^{11}BH_4)_3$

Angelina Gigante[1,2], Seyedhosein Payandeh[2], Jakob B. Grinderslev[4], Michael Heere[5], Jan Peter Embs[3], Torben Jensen[4], Tatsiana Burankova[3], Arndt Remhof[2], Hans Hagemann[1*]

[1]Département de Chimie-Physique, Université de Genève, 1211 Geneva 4, Switzerland

[2]Empa, Swiss Federal Laboratories for Materials Science and Technology, 8600 Dübendorf, Switzerland

[3]Laboratory for Neutron Scattering and Imaging, Paul Scherrer Institute, 5232 Villigen PSI, Switzerland

[4]Interdisciplinary Nanoscience Center (iNANO) and Department of Chemistry, Aarhus University, Langelandsgade 140, DK-8000 Aarhus C, Denmark

[5]Institute for Applied Materials – Energy Storage Systems (IAM – ESS), Karlsruhe Institute of Technology (KIT), Eggenstein-Leopoldshafen, Germany

(*) Hans-Rudolf.Hagemann@unige.ch

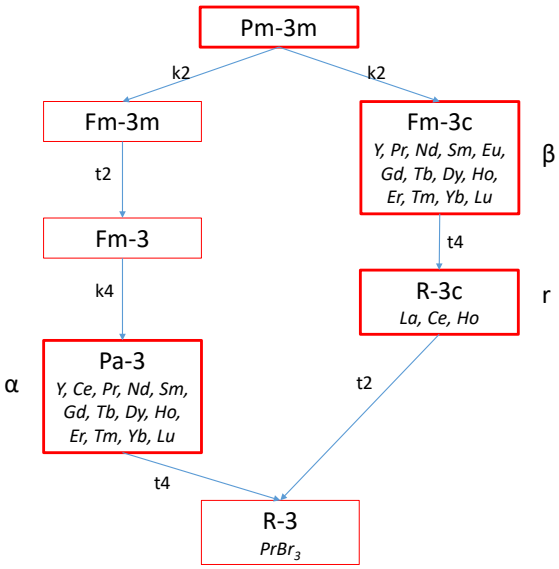

Fig. S1. Space groups observed for $RE(BH_4)_3$ and their group-subgroup relation (t translationsgleich, k klassengleich). These space groups are also related to the space group R-3 observed for $PrBr_3$.

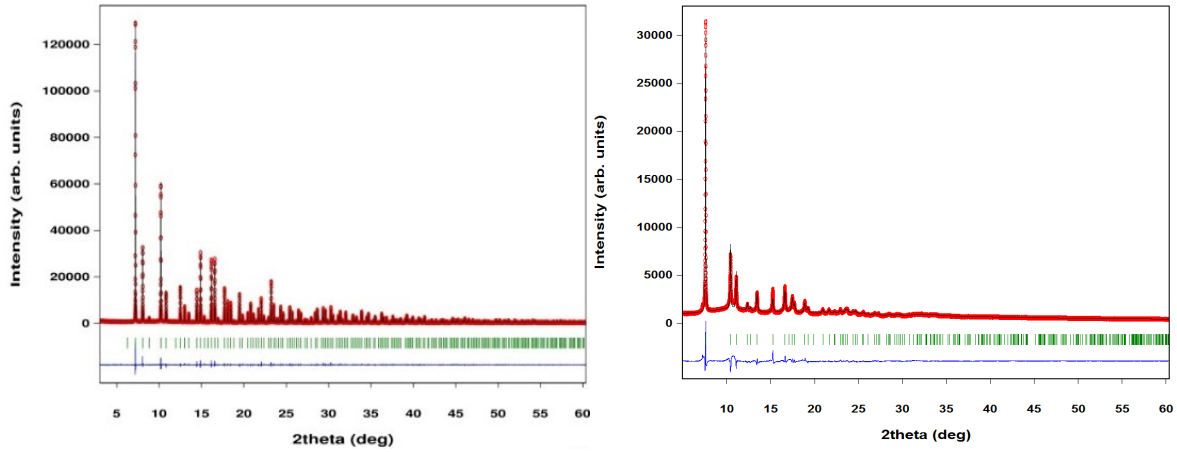

Fig. S2. a) Rietveld refinement of α-Pr($^{11}BH_4$)$_3$ phase in Pa-3 with Rwp = 3.52, χ^2=4.62 (300K) and b) Rietveld refinement of r-Pr($^{11}BH_4$)$_3$ phase in R-3c with Rwp=5.5, χ^2=17.1 (319K, after heating and cooling).

Table S1. Symmetry analysis of the vibrations of $Gd(BH_4)_3$ in the Pa-3 space group from Sato *et al.* The frequencies corresponding to ν_4 and ν_2 are highlighted in blue and red respectively [1].

Modes	**Frequencies**									
Ag	47	154	193	254	356	548	579	1073	1081	1103
	1147	1296	2287	2293	2320	2339				
Eg	43	167	190	259	373	545	582	1062	1094	1100
	1155	1285	2276	2306	2318	2333				
Tg	41	56	74	128	147	166	188	199	218	228
	269	274	368	378	445	534	537	544	579	584
	589	1063	1065	1068	1086	1089	1096	1099	1101	1104
	1147	1154	1194	1281	1288	1299	2270	2273	2280	2301
	2306	2310	2315	2319	2334	2335	2342	2345		
Au	116	161	202	296	462	540	587	1062	1098	1104
	1204	1272	2268	2318	2336	2350				
Eu	116	154	195	233	376	534	583	1067	1089	1100
	1151	1297	2275	2303	2315	2337				
Tu	61	74	117	150	172	191	199	219	236	259
	278	364	374	393	534	543	546	578	582	589
	1061	1066	1069	1085	1092	1096	1099	1102	1104	1148
	1156	1174	1282	1292	1295	2271	2272	2278	2299	2307
	2310	2317		2319	2329	2333	2337	2343		
Tu	61	75	117	150	179	197	208	219	236	260
	278	365	393	424	534	543	546	578	582	589
	1061	1067	1069	1091	1092	1096	1099	1102	1104	1150
	1173	1185	1282	1292	1295	2271	2273	2278	2305	2310
	2317	2318	2328	2332	2334	2340	2344			

6 Raman active translational and 6 Raman active librational modes are predicted in $Pr(^{11}BH_4)_3$ in the R-3c phase. Globally, there are much fewer Raman active lattice modes in $Pr(^{11}BH_4)_3$ in the R-3c phase than the Pa-3 phase (see Tables S2 and S3).

Table S2. Symmetry analysis of the vibrations of $Pr(^{11}BH_4)_3$ in the Pa-3 phase. The frequencies corresponding to ν_4 and ν_2 are highlighted in blue and red respectively.

	A_g	E_g	T_g	A_u	E_u	T_u	
Pr	1	1	3	1	1	3	Translational lattice modes
B	3	3	9	3	3	9	Translational lattice modes
ν_1	1	1	3	1	1	3	Internal A_1 mode
ν_2	2	2	6	2	2	6	Internal E mode
ν_3	3	3	9	3	3	9	Internal T_2 mode
ν_4	3	3	9	3	3	9	Internal T_2 mode
lib	3	3	9	3	3	9	Libration (T_1 symmetry)

Table S3. Symmetry analysis of the vibrations of $Pr(^{11}BH_4)_3$ in the R-3c phase.

	A_{1g}	A_{2g}	E_g	A_{1u}	A_{2u}	E_u	
Pr	0	0	0	1	1	2	Translational lattice modes
B	1	2	3	1	2	3	Translational lattice modes
ν_1	1	0	1	1	0	1	Internal A_1 mode
ν_2	2	0	2	2	0	2	Internal E mode
ν_3	1	2	3	1	2	3	Internal T_2 mode
ν_4	1	2	3	1	2	3	Internal T_2 mode
lib	1	2	3	1	2	3	Libration (T_1 symmetry)
	6	6	12	6	6	12	Total internal + libration modes

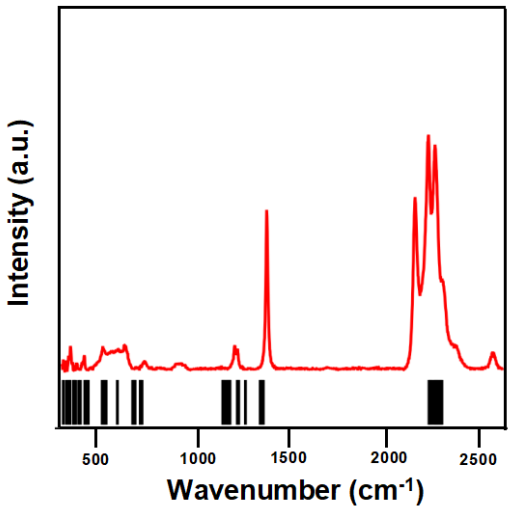

Fig. S3. Comparison of the Room temperature Raman spectrum of $Pr(^{11}BH_4)_3$ (red spectrum) with the calculated spectra of $Gd(BH_4)_3$ (black lines) [1].

Table S4. Summary of the Neutron Cross Sections of the studied species. σ_{abs} is given for neutrons with wavelength of 4.0Å. 1b= $10^{-28}m^2$.

Species	$\boldsymbol{\sigma_{scat}}$**[b]**	$\boldsymbol{\sigma_{abs}}$**[b]**	$\boldsymbol{\sigma_{inc}}$**[b]**	$\boldsymbol{\sigma_{coh}}$**[b]**	$\frac{\boldsymbol{\sigma_{inc}}}{\boldsymbol{\sigma_{scat}}}$ **[%]**
$Pr(^{11}BH_4)_3$	1004.0	34.5	964.2	40.4	96.0
12H	984.0	8.9	963.6	21.1	97.9
3 ^{11}B	17.3	0.0	0.6	16.7	3.5
Pr	8.0	76.8	0.1	7.9	1.3

S_{BH4} can be defined as follow:

$$S_{BH4}(Q,E) = S_{vib}^{BH4}(Q,E) \otimes S_{loc}^{BH4}(Q,E) = digl, BH4 \quad (S1)$$

Taking into account that experimental spectra are normally corrected for the detailed balance factor $DBF = e^{-\frac{E}{2k_BT}}$ on the step of the data reduction, we will consider only classical (symmetric in energy) expressions for the individual dynamic structure factors. In addition to the lattice vibrations observed in the inelastic spectrum of $Pr(^{11}BH_4)_3$ at 7.5, 16 and 23meV as shown in Fig. S4, there is an excess of phonon density of states in the low-energy range (<2meV) as compared to the quadratic dependence on energy predicted by the Debye theory for acoustic vibrations in crystalline solids. This feature is prominent in quasi-harmonic crystals pointing to intrinsic disorder in the system [2-4]. This low-energy inelastic broad band can be modeled with a Lorentzian curve with the amplitude depending on the average mean square displacement as follows [4]:

$$S_{vib}^{BH4}(Q,E) = exp(-\langle u^2\rangle Q^2)\left\{\delta(E) + [exp(\langle u^2\rangle Q^2) - 1]\frac{1}{\pi}\frac{\Gamma}{\Gamma^2+E^2}\right\} \text{(S2)}$$

where $\sqrt{\langle u^2\rangle}$ is the vibrational mean square displacement, $\Gamma = \hbar/\tau_{lib}$ is the half width at half maximum (HWHM) of the quasielastic line. Assuming that BH_4^- groups perform tumbling motions around their C2/C3 axes of symmetry, the scattering function $S_{loc}(Q,E)$ reads [5, 6].

$$S_{loc}(Q,E) = \frac{1}{4}\left(1 + 3j_0(QR_{H-H})\right)\delta(E) + \frac{3}{4}\left(1 - j_0(QR_{H-H})\right)\frac{4\hbar/\tau_0}{E^2+\left(4\hbar/\tau_0\right)^2} \text{(S3)}$$

where j_0 is the spherical Bessel function of the 1-th order, $1/\tau_0$ is the jump rate around one C2/C3-axis (Note that $1/\tau$ in the work by Sköld is the total probability per unit time for a jump around any axis, whereas in the current and previous works $1/\tau_0$ is the jump rate around one selected axis [5, 6]. The relaxation times are related as $\tau_0=3\tau$. $R_{H-H} = \frac{2\sqrt{2}}{\sqrt{3}}R$ is the average distance between two hydrogens in the borohydride tetrahedra with the B-H bond length R. Finally, equations S2-S3 are combined in equation S1 and the resulting dynamic structure factor is convoluted with the resolution function of the instrument, R(Q,E).

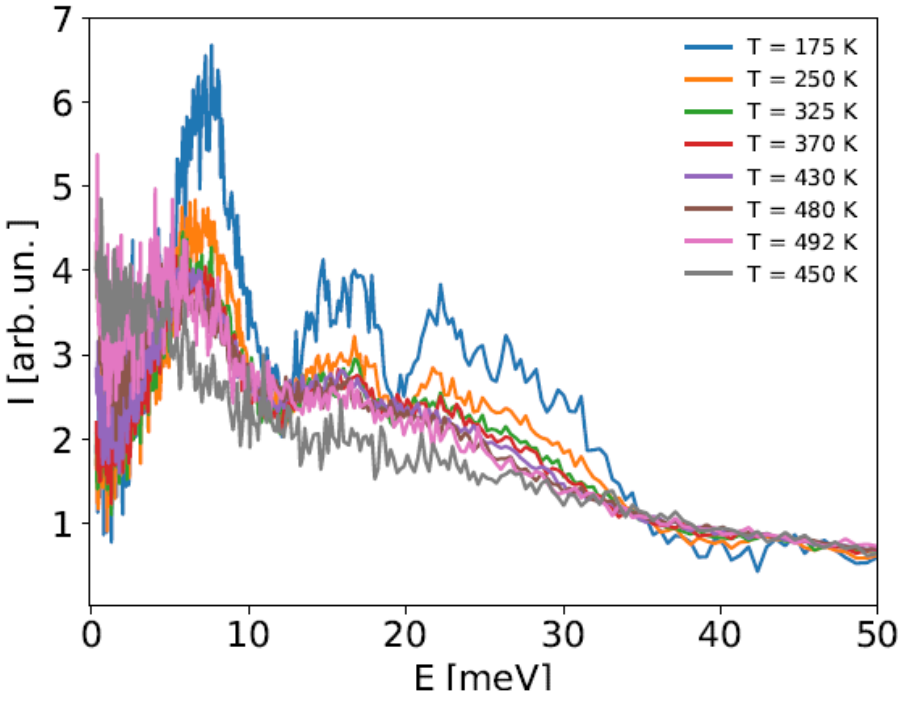

Fig. S4. PDOS of hydrogen for $Pr(^{11}BH_4)_3$ at different temperatures. Upon heating the band at 7.5meV shifts to lower energies, the other two bands become broader, as well as their intensities relative to the first band decrease. The changes of the inelastic spectrum upon the phase transition at 495K are irreversible.

References

1. Sato T, Miwa K, Nakamori Y, Ohoyama K, Li H-W, Noritake T, et al. Experimental and computational studies on solvent-free rare-earth metal borohydrides $R(BH_4)_3$ (R=Y, Dy, and Gd). Physical Review B, 77, 2008, pp. 104114.
2. Buchter F, Łodziana Z, Mauron P, Remhof A, Friedrichs O, Borgschulte A, et al. Dynamical properties and temperature induced molecular disordering of $LiBH_4$ and $LiBD_4$. Physical Review B, 78, 2008, pp. 094302.
3. Duchêne L, Lunghammer S, Burankova T, Liao W-C, Embs JP, Copéret C, et al. Ionic Conduction Mechanism in the $Na_2(B_{12}H_{12})_{0.5}(B_{10}H_{10})_{0.5}$ closo-Borate Solid-State Electrolyte: Interplay of Disorder and Ion–Ion Interactions. Chemistry of Materials, 31, 2019, pp. 3449-60.
4. Lechner RE. II Instrumentation II. 3 Quasielastic and Inelastic Neutron Scattering. Neutrons in Soft Matter, 2011, pp. 203.
5. Sköld K. Effects of Molecular Reorientation in Solid Methane on the Quasielastic Scattering of Thermal Neutrons. The Journal of Chemical Physics, 49, 1968, pp. 2443-2445.
6. Burankova T, Duchêne L, Łodziana Z, Frick B, Yan Y, Kühnel R-S, et al. Reorientational Hydrogen Dynamics in Complex Hydrides with Enhanced Li^+ Conduction. The Journal of Physical Chemistry C, 121, 2017, pp. 17693-17702.